

## Near infrared astronomy with moderate size telescopes <sup>1</sup>

T. N. Rengarajan

*Tata Institute of Fundamental Research, Homi Bhabha Road, Mumbai 400 005, India*

**Abstract.** Observations in the near-infrared (NIR) band have become a regular feature of all observatories in the world. There are several NIR bands that are accessible to ground based telescopes situated at modest altitudes. Such observations address a gamut of astrophysical problems ranging from the solar system, Milky Way to external galaxies. The lower extinction in the NIR enables one to observe objects deeply embedded in clouds that cannot be observed in the optical band. There are also several NIR lines that are valuable diagnostics of physical conditions. Even in this era of large telescopes, modest size (1-2 m) telescopes can be very valuable for a variety of observations. In this talk, I will briefly review some technical aspects and describe some interesting photometric, polarimetric and spectroscopic observations from the literature as examples of what can be done using Indian telescopes.

*Key words* : infrared : general - telescope

### 1. Introduction

The earth's atmosphere has many windows that are transparent in the near infrared (NIR) - J, H, K, L, M bands with central wavelengths of 1.2, 1.6, 2.2, 3.5 and 4.8  $\mu\text{m}$  respectively. In recent years, great improvements in infrared detectors have made this window a vibrant tool in several astrophysical areas. Unlike the optical CCD detectors, NIR detector sensitivities are mainly determined by the background photon noise due to the emission from the atmosphere, telescope mirror etc. The low background in the JHK bands make them an ideal choice for high sensitivity studies. Further, high sensitivity observations can be undertaken even from modest altitude sites whereas observations in the L and M bands require good high altitude sites. In the rest of my talk I will mostly confine myself to the JHK bands. In the next two sections, I will briefly describe the advantages of the NIR band and some aspects of the 2D arrays and the observational considerations. In the last section some interesting results obtained using the NIR window will be presented.

---

<sup>1</sup> Presented at the UPSO 104 cm Telescope Silver Jubilee Workshop on Astronomy with Moderate Sized Optical Telescopes.

## 2. Advantages of NIR observations

Apart from considerably extending the optical window, the NIR band allows one to probe objects and regions embedded in high density material. This arises from the considerably low extinction in the NIR as compared to the visual. For example, one can probe in the K band, regions of optical extinction  $A_V$  ranging from 10 to 30. This is particularly important to study regions of star formation deeply embedded in molecular clouds, dense central regions of galaxies and AGNs. The NIR band is also very useful in the study of cool stars, post AGB stars, mass loss stars etc. wherein the emission peaks in this window. NIR spectral lines provide new handles to study the physical conditions of the material in a variety of astrophysical situations. Again, it is particularly useful for regions of high extinction. In extragalactic studies NIR window is the ideal choice for the study of high red shift objects since many of the optical lines are red shifted into this window. Large statistical study of high red shift objects can also be conveniently undertaken using photometric studies in the NIR band. Finally, NIR observations provide the much needed spectral extension from the optical for the study of non thermal spectra of a variety of objects. Apart from the above fields, NIR observations will be particularly useful for the study of planetary atmosphere, comets, brown dwarfs, supernovae, lensed galaxies and dust features. One may also note that loss of resolution from atmospheric turbulence (seeing) is less at NIR wavelength as compared to the visual; hence it is possible to improve spatial resolution with relatively simple techniques like co-adding, tip-tilt corrections etc. The other advantage of the J, H and K windows is in the study of lunar occultations. The scattered background light due to the moon at these wavelengths are negligible in comparison to the optical region. At the same time the thermal contribution due to moon itself is negligible.

## 3. Technical aspects

### 3.1 Infrared array detectors

In recent years there has been a dramatic improvement in the availability and sensitivity of two dimensional infrared arrays. They are fast catching up with the CCD arrays. Arrays with  $512 \times 512$  elements are in use and larger ones are on the way. Table 1 lists some properties of Si(CCD) and infrared detector materials. The two most commonly used materials are InSb and HgCdTe; both have high quantum efficiency and low read noise. PtSi has a low quantum efficiency of 5 - 10%; however, it is available in a large format useful for imaging large bright objects. Table 2 lists some characteristics of three different arrays for a comparison. It may be noted that both InSb and HgCdTe arrays can be used in JHK bands while for L and M bands only the former can be used. HgCdTe array can operate at solid nitrogen temperature whereas InSb array is best operated at 30-40 K requiring cooling with liquid helium or closed cycle helium gas cooler.

**Table 1.** Properties of near infrared detector materials.

Material	Band Gap (eV)	$\lambda_c$ ( $\mu\text{m}$ )	Operating Temp. ( $^{\circ}\text{K}$ )
Si (CCD)	1.1	1.0	150-170
Ge	0.7	1.7	77-100
HgCdTe	0.5	2.5	60-77
PtSi	0.25	5.0	40-60
InSb	0.23	5.4	30-40
Si:In	0.18	7.0	30-40

**Table 2.** Near infrared arrays.

	Hughes PtSi	Rockwell NICMOS3	SBRC InSb
	256 $\times$ 256	256 $\times$ 256	256 $\times$ 256
Pixel ( $\mu\text{m}$ )	30	40	30
Fill Factor	87%	90%	97%
Readout Type	Direct-switched MOSFET	CMOS-switched FET	Direct PMOS- switched FET
Dark Current ( $\text{e}^-/\text{s}$ )	<10	<5	<45 (50K) <1 (35K)
Read Noise ( $\text{e}^-$ )	<60	<20	<50
Q.E.	3-10%	>50%	80-90%

Infrared arrays, unlike CCD do not have a direct read out; they are generally, bump bonded to another read out device. This leads to increased read noise as well as some loss of robustness. However, read noise can be reduced by correlated multiple read out technique. Further, it is possible to directly address any wanted pixel.

### 3.2 Telescope aspects

As remarked earlier photon noise resulting from background emission is the main limit to sensitivity in the infrared. One would, therefore, like to have low emissivity mirrors. However, in the JHK bands even conventional optical telescopes are usable since the background emission reduces exponentially in this wavelength range. This also makes even 2 km sites suitable for JHK bands. In fact, the gain is only marginal at much higher sites. However, observations in L and M bands gain significantly by using well designed infrared telescope at high and cold sites. With the advent of arrays, secondary chopping is not essential for JHK bands. Carefully designed cold mask in the cold optical train of the NIR photometer can mostly eliminate the emission from high emissivity edges, spiders etc. For any infrared telescope it is important to keep the mirrors dust free by periodic cleaning.

#### 4. Examples of scientific results from NIR observations

In recent years there has been an explosive growth of scientific results using NIR arrays. An idea of the variety of topics covered can be had from proceedings of various meetings. In particular, one may refer to *Infrared Astronomy with Arrays: the Next Generation* (Ed. McLean, 1994) and *Clouds, Cores and Low Mass Stars* (Eds. Clemens and Barvainis, 1994). Here, I will give a few examples of observations using modest sized telescopes.

##### 4.1 Photometric imaging

Photometric imaging has been extensively used to study stars embedded in molecular and dark clouds. Our understanding of low mass star formation has been considerably enhanced by these observations. Various techniques like colour-colour diagrams and IR spectral features have been used to identify the nature of PMS objects. Charles Lada and collaborators have carried out extensive studies of several star forming complexes. In Fig. 1 is shown the contour plot of surface density of stars detected in K band towards NGC 1333 region (Lada, Alves & Lada 1996). It is seen that the stars are strongly clustered; further, the clustered stars also exhibit a larger fraction of

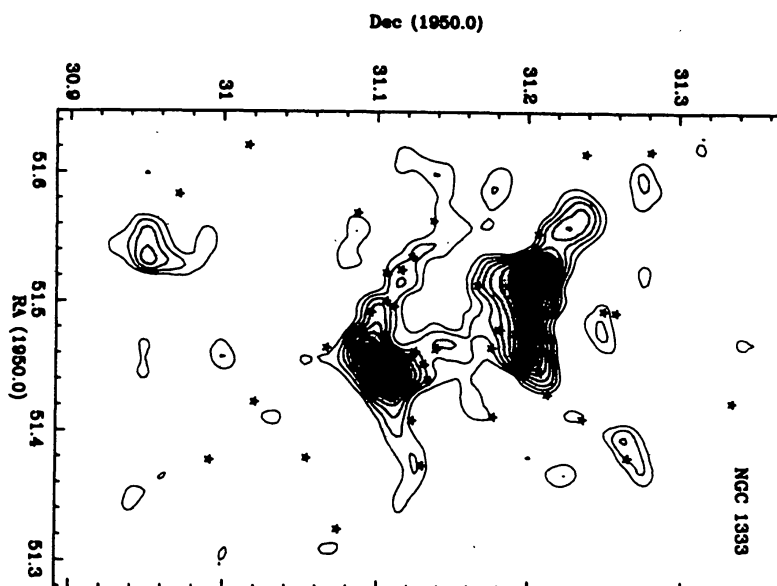


**Figure 1.** Contour map of surface density of stars detected in K band towards NGC 1333. Filled stars mark the location of IR excess stars which are seen to strongly cluster (Lada, Alves & Lada, 1996).

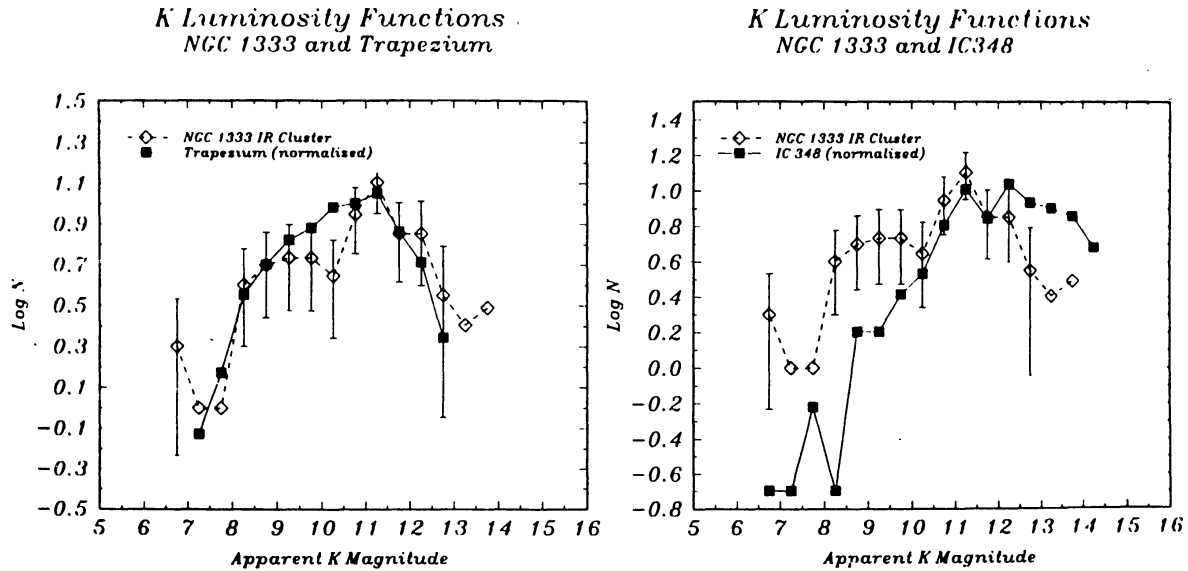


**Figure 2.** Comparison of the normalised de-reddened differential KLF of NGC 1333 that for the Trapezium cluster and IC 348 (Lada et al, 1996).

IR excess stars as compared to the foreground/background stars. K band luminosity function (KLF) has been studied for several clusters and by model fitting, discrimination can be made between coeval star formation and continuous star formation (CSF). It is found that while the coeval model fits the Trapezium cluster better, for IC 348 the CSF model is better (Lada 1994). Fig. 2 taken from Lada, Alves & Lada (1996) shows the comparison of differential KLF for three clusters-NGC 1333, Trapezium and IC 348. The shape of NGC 1333 KLF is very similar to that of Trapezium, but differs from that of IC 348. This is interpreted to indicate that the age of NGC 1333 is similar to that of the Trapezium ( $\sim 10^6$  yrs) and significantly less than that of IC 348 ( $5 - 7 \times 10^6$  yrs).

NIR imaging of external galaxies is becoming a valuable tool to study morphological structures and star formation history in external galaxies. Fig. 3 shows K band surface brightness profile of UGC 4020 observed as a part of UGC sample of galaxies (Rieke 1994). Also shown in the figure are the profiles of ellipticity and major axis position angle. This galaxy displays a twist in its isophotes as seen in the major axis profile and a change in ellipticity in the transition region of bulge to disk.

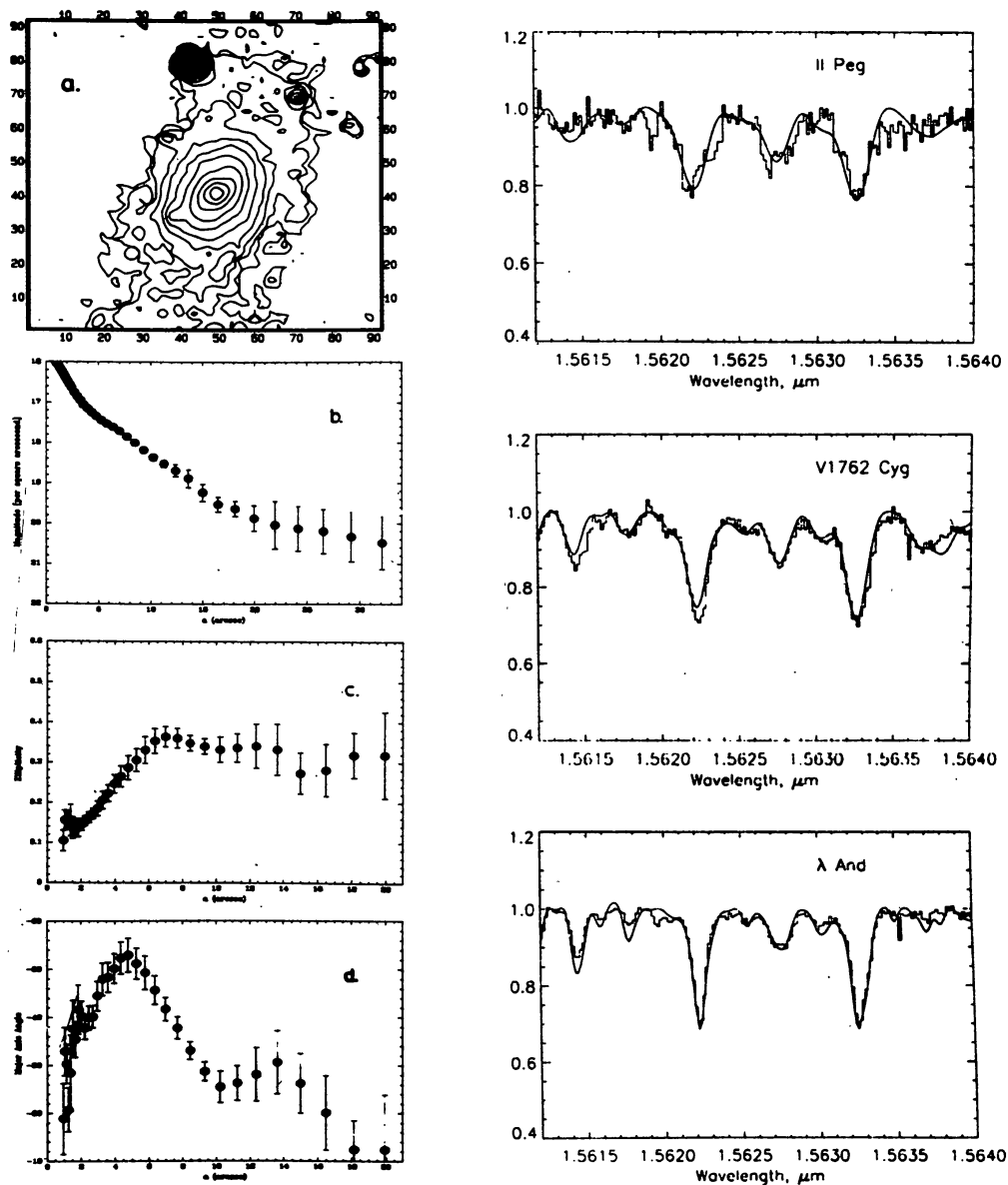


**Figure 3.** (a) Contour plot of UGC 4020 at K. (b) Surface magnitude profile in K magnitude per square arcsecond. (c) Profile of ellipticity o fitted surface brightness (d) Position angle of the major axis for fitted ellipses (from Rieke, 1994).

**Figure 4.** (right) Best fits (solid lines) to the spectra of spotted stars. The non spot temperature (K), spot temperature (K) and the fraction of spotted surface area are : 4800, 3550 & 0.48 for II peg; 4600, 3474, 0.3 for V1762 Cyg; 4775, 3650, 0.21 for λ And respectively (from O'Neal & Neff, 1997).

## 4.2 Spectral studies

There are several spectral lines in the NIR band that are valuable diagnostics of physical conditions. Spectral studies have proved valuable in a variety of objects and environments. An interesting use of NIR spectral line is the study of star spots in active stars by O' Neal & Neff (1997). They have made use of a pair of vibrational-rotational absorption lines of the OH molecule near  $1.563 \mu\text{m}$ . As compared to the use of optical TiO bands, the IR lines have more contrast with respect to photospheric emission, can be used for stars at temperatures as high as 5000 K and are also in a region of low atmospheric background. Fig. 4 taken from the above work shows the fits obtained for three spotted stars and the spot parameters obtained. Clearly, the technique greatly increases the range of star spot temperatures that can be studied.

High resolution NIR imaging of Orion in the emission lines of  $\text{H}_2$  ( $2.122 \mu\text{m}$ ) and [FeII] ( $1.644 \mu\text{m}$ ) has contributed to our understanding of shocked molecular outflow (Allen & Burton 1993). Many Herbig-Haro objects are seen as [FeII] high velocity bullets at the heads of wakes of  $\text{H}_2$  emitting gas. This is illustrated in Figs. 5a & b (Tedds et al. 1994). Imaging spectroscopy has been developed into a powerful technique at the Anglo Australian Telescope to map simultaneously

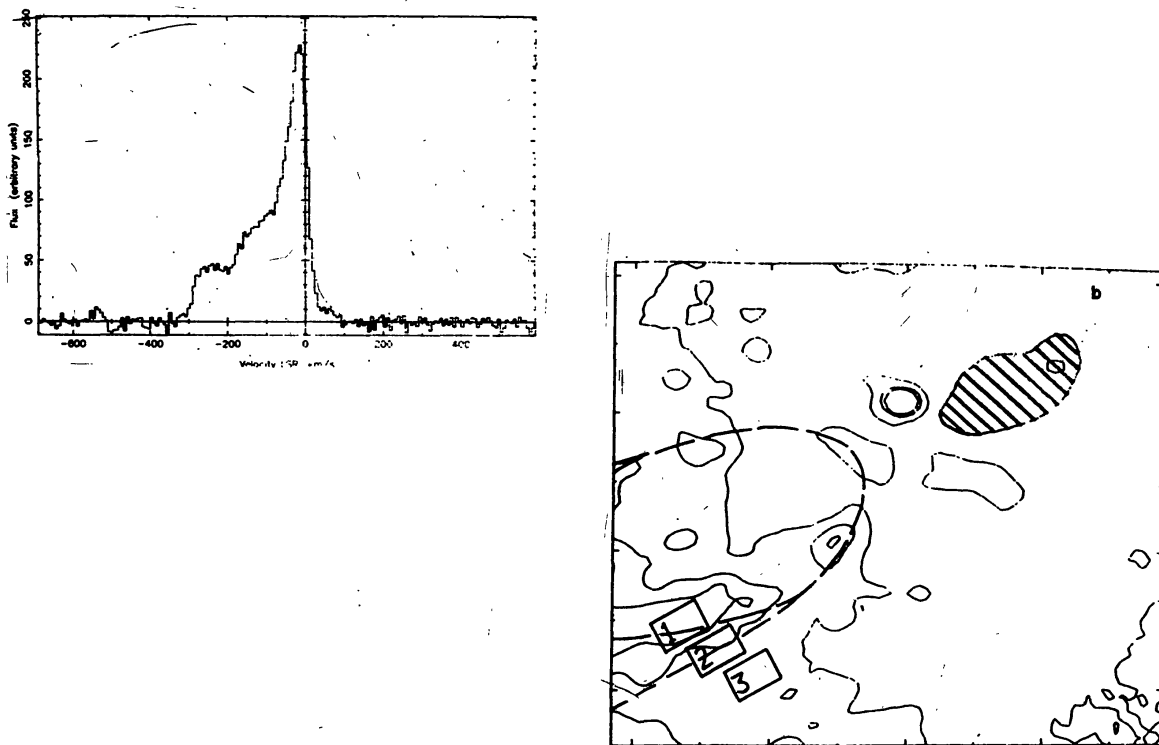
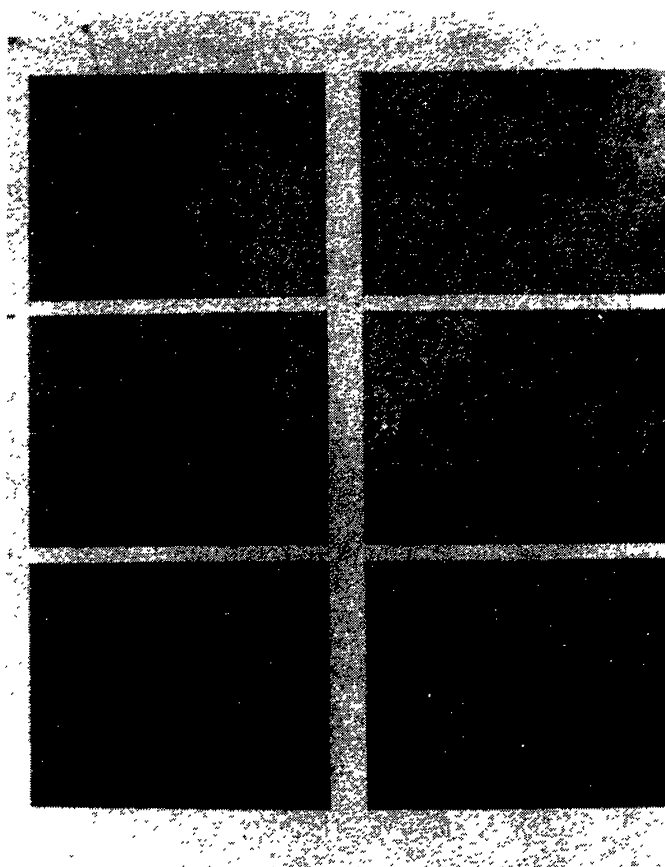


Figure 5. a). [FeII]  $1.644 \mu\text{m}$  integrated velocity profile for M42 HH1.

b)  $\text{H}_2$  1-0 S(1)  $2.122 \mu\text{m}$  contour plot of M42 HH1. The shaded area indicates the position of [FeII] bullet, dashed line indicates an idealised bow-shock wake. Line profiles across the wake (numbered locations) show change from double peaks to a single peak (from Tedds et al., 1994).



**Figure 6.** Spectrophotometric slit scan maps of  $2 \times 2.5$  arcminute region of Galactic Centre in different lines.

Top left :  $\text{Br}\gamma$ : thermal filaments seen. Top centre :  $\text{H}_2$  S(1) line at  $2.122\mu\text{m}$ . The Interface between the two emission regions indicates intrusion of ionized surface into the molecular ring. Top right : He I  $2.058 \mu\text{m}$  emission showing in particular helium emission stars. Bottom left :  $[\text{FeIII}]$   $2.217 \mu\text{m}$ ; maximum intensity in the  $\text{Br}\gamma$  cavity. Bottom centre and right : stars with little CO absorption and deep CO absorption. The two populations have very different distributions (from Allen, 1994).

in several spectral lines. Fig. 6, taken from Allen (1994) shows maps of  $2 \times 2.5$  arcminute region centred on the Galactic Centre in different spectral lines. The figure caption highlights the major results.

Greene and Lada (1996) have undertaken  $1.15 - 2.42 \mu\text{m}$  spectroscopic survey of about 100 YSOs. They find that the strength of several atomic and CO absorption features are closely related to the spectral energy distribution, with the absorption decreasing from the least obscured class III phase to the most obscured class I phase implying a systematic increase in veiling from underlying photosphere. The increase in the veiling is mostly due to increased emission from the luminous circumstellar material.



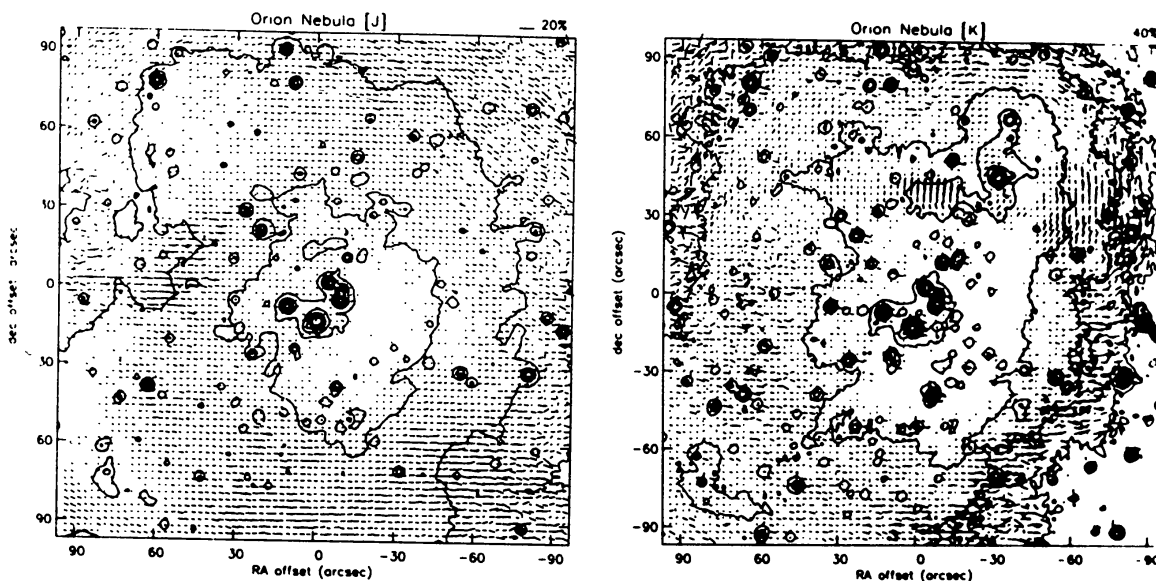


**Figure 7.** The Orion nebula in J band (left) and K band (right). Trapezium is roughly at the centre. The plotted vectors are the position angle and amplitude of polarization. In the K map, the prominent BN object is at (RA, dec) offsets of (-30, +48); IRC2 is  $\sim 8''$  SE of BN near the centre of symmetry of the predominant polarization pattern.

### 4.3 Polarization studies

Polarization arising from scattering by dust is a powerful technique to probe the environment of embedded objects. Fig. 7 shows the J and K broad band and polarimetric images of BN/IRC2 and Trapezium regions of OMC-1 obtained by Weintraub et al. (1994). One sees differences in the emission peaks and the scattering centres mapped by the polarization vector patterns in the two bands. A detailed study of these differences leads to an understanding of the energizing sources and the material structure. For more details, the paper quoted above may be referred to. Sogawa et al. (1997) have also shown that polarization patterns can be effectively used to discriminate between objects belonging to a cluster and unassociated background stars.

### References

- Allen D. A., 1993, *Nature*, 363, 54.
- Greene T. P., Lada C. J., 1996, *AJ*, 112, 2184.
- Lada E. A., 1994, in *Clouds, Cores and Low Mass Stars*, eds. D. P. Clemens & R. Barvainis, ASP Conference Series, Vol. 65, p. 401.
- Lada C. J., Alves J., Lada E. A., 1996, *AJ*, 111, 1964.
- O' Neal D., Neff J. E., 1997, *AJ*, 113, 1129.
- Rieke M. J., 1994, in *Infrared Astronomy with Arrays : The Next Generation*, ed. I. S. McLean, Kluwer, p. 21.
- Sogawa H., Tamura M., Gatley I., Merrill K. M., 1997, *AJ*, 113, 1057.
- Tedds J. A., et al., 1994, in *Clouds, Cores and Low Mass Stars*, eds. D. P. Clemens & R. Barvainis, ASP Conference Series, Vol. 65, p.375.
- Weintraub D. A., Kastner J. H., Lowrance P., 1994, *ibid*, p. 266.